Monitoring Joint Penetration Using Infrared Sensing Techniques

Sensing the surface temperature of the plates being welded may lead to adaptive control of joint penetration

BY W. CHEN AND B. A. CHIN

ABSTRACT. The objective of this research is to apply infrared sensing and computer image processing techniques to improve the welding process through dynamic control of joint penetration parameters. A front side scanning infrared camera was used to monitor molten pool and surface temperature distributions surrounding the pool during the welding process. Welding parameters were varied to change the depth of penetration and the corresponding changes in the temperature distributions recorded. A linear relationship between bead width of weld and infrared thermal image profile width was established. Additionally, the depth of joint penetration was found to be a function of the area under the measured surface temperature profile taken at the centerline of the molten metal pool. These results suggest that information from the surface temperature of plates being welded may be used to monitor and control the depth of penetration and bead width in real time.

Introduction

With continual advances in digital and sensor technology, new methods of identifying perturbations during the welding process with relatively high accuracy have become possible. Arc position, part placement variations, surface contamination and joint penetration are key variables that must be controlled to insure satisfactory weld production. The varied nature of these parameters have made it difficult to adaptively control the welding process. Arc position or joint tracking has been the most highly pursued adaptive control with several methods marketed commercially with limited success. Previous attempts to monitor joint penetration have required backside sensors or relied upon an optically measured bead width and known bead width to penetration relation to control weld joint penetration (Refs. 1-4). One particular difficulty with the latter technique is that minor changes in material composition (heat-to-heat variation or tramp element concentrations) have been shown to alter dramatically penetration behavior (Refs. 5-7). This paper presents results of a set of experiments designed to measure surface temperature distributions (differences in surface temperature in different regions) during the production of welds with various degrees of penetration. Conclusions drawn from these data and previous results (Refs. 8-10) may provide the needed information required to automate penetration control.

During the welding process, the high temperatures associated with the arc and appropriate thermophysical properties such as thermal diffusivity cause strong spatial temperature gradients to occur in the region of the weld pool. Convection in the weld pool, shape of the weld pool and heat transfer in both the solid and liquid metal determine the temperature distributions in the plate and on the surface. For an ideal weld with constant conditions, these surface temperatures should show repeatable and regular patterns. Perturbations in welding penetration should be clearly identifiable from variations in the surface temperature distributions (Ref. 10). Control of penetration variations due to minor differences in impurity element levels should be possible since downward and radial convection patterns, which have been shown to be responsible for variable joint penetration, would be clearly identified through differences in the molten pool temperature distribution.

Modern infrared thermography equipment allows rapid measurement of surface temperature distributions. This technique provides an ideal way of monitoring perturbations in the weld process, providing that the plate surface and weld pool are visible to the sensing device. The principal limitation to this type of sensing is its currently prohibitive cost. However, new inexpensive CCD sensors (charge coupled devices) are currently being developed that should be commercially available within the next five years for sensing applications.

The objective of the series of experiments presented in this paper is to relate the depth of joint penetration and bead width to measurable surface temperature distributions. Measurements of the bead width and depth of penetration were compared with magnitude, gradient, area under thermal profile, and symmetry of the infrared sensed temperature distributions.

KEY WORDS

Weld Monitoring
Penetration Monitor
Infrared Sensing
Computer Image
Front-Side Scanning
Thermal Image Profile
Surface Temperature
Weld Bead Width
Joint Penetration Depth
Infrared Detector

Experimental Procedure

All experiments in this investigation were conducted using gas metal arc welding (GMAW). The material was AISI 1008 steel with all plates 30.48 × 15.24 cm (12 × 6 in.) in size. Two standard thicknesses of steel plates were milled to produce a precise butt joint fit. The surfaces of these edges were then prepared for welding using standard preparation techniques. Figure 1 shows the experimental setup used to perform the welds. All welds were made with an ESAB Model LAH 315P pulse arc power source with a water-cooled welding gun and ESAB A10-MEC44 wire

W. CHEN is a Graduate Research Assistant and B. A. CHIN is a Professor in Materials Engineering, Auburn University, Auburn, Ala.

Paper presented at the 69th Annual AWS Meeting, held April 17-22, 1988, in New Orleans, La.

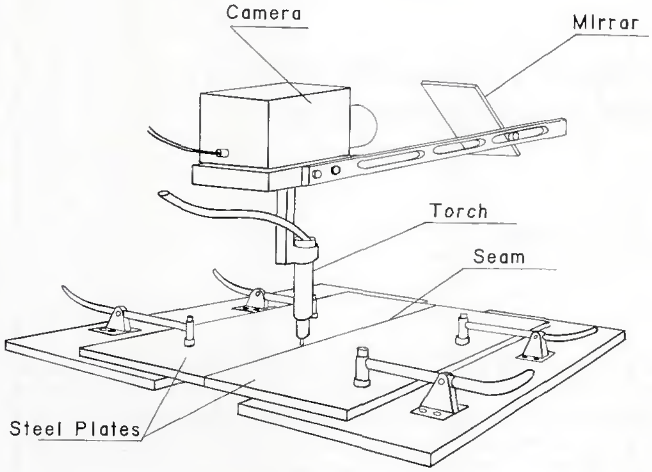

Fig. 1—Schematic of experimental setup used to produce welds. A front-side reflecting mirror is used to reflect IR radiation into horizontally mounted camera.

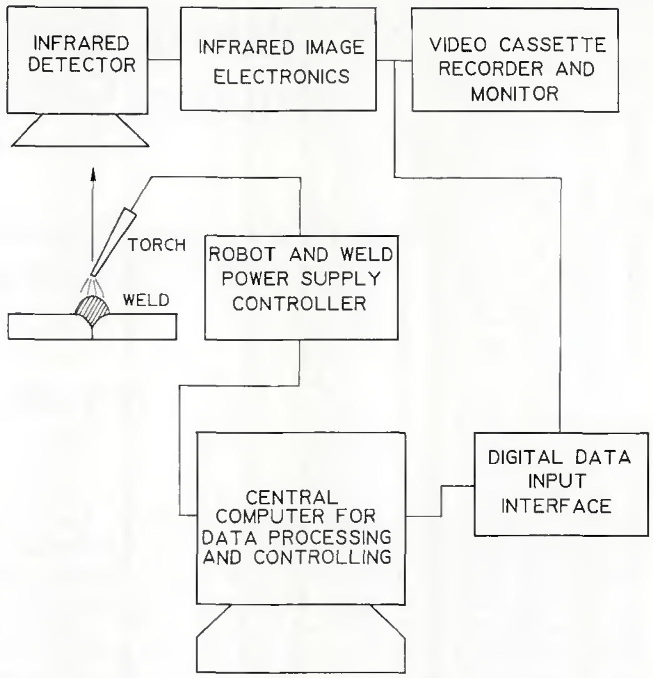

Fig. 2—Block diagram of the data-acquisition and control system.

feed unit. Welding wire of designation ER70S-3 of 0.138 cm (0.35 in.) diameter was used. Current output of the power source was measured using a Columbia Electric clamp-on ammeter with a scale of 200 A. Welds were produced using DC power, and a shielding gas of argon-2% oxygen at a 1.8 cm^3h^{-1} (30 cfh) flow rate. The welding gun was mounted to a Health Engineering Co. x-y positioning table (Model ICD 600-MODFD), which is controlled through a Hewlett Packard Series 320 microcomputer. A constant travel speed of 2.3 cm/min (0.9 in./min) was used in all experiments. Arc currents of 60 to 155 A at arc voltages of 18 to 32 V DC were used.

Surface temperature distributions were measured using an infrared scanning camera placed for front-side viewing of the welded plates. The camera unit, manufactured by Inframetrics Corp., converts the invisible infrared radiation given off by the weld pool and surrounding regions, which are heated during the welding process, into equivalent voltage signals that represent the plate temperature distributions. The infrared-sensitive detector consists of a mercury, cadmium, telluride (Hg-Cd-Te) photovoltaic cell, sensitive in the spectral range of 8 to 12 μm. The signals are then amplified and transferred via interconnecting cables to a video display unit, video tape recording unit and interface of the processing computer used for acquisition and analysis of the surface temperature information. Figure 2 is a block diagram of the data-acquisition and feedback control system.

The computer with custom data-acquisition interface and programs receives the thermal profiles in frames consisting of 192 × 251 discrete temperature measurements from the infrared camera corresponding to one scan of the plate surface. The scanning rate of the camera is 30 frames per second (fps), with data acquisition by the computer being 20 fps without digital storage and 10 fps if the data are stored in digital array for future analysis and processing. Software programs have been generated that can be used to display during the welding process the temperature information in two-dimensional isotherm plot (temperature as represented by color vs. x and y coordinates on the plate surface) or linear line scans (temperature profiles of a given line perpendicular to the welding gun direction). The equipment can be programmed so that two-dimensional temperature displays are shown on the computer video monitor and line scans displayed on a secondary video monitor and recorded for later study. During the welding process, the position of the infrared camera was fixed relative to the welding gun to provide measurement of temperatures in the weld pool and its vicinity. Experimental conditions were carefully maintained to minimize possible errors from uncontrolled variations.

Measurement of joint penetration and bead width were performed after welding using standard metallographic techniques. Sections were cut from the weld, which corresponded to the exact position of the weld where the temperature measurements were taken. Molten pool-solid metal interfaces and heat-affected zone interfaces were measured from metallographic samples that were polished and then etched using a 4% nitric acid and 96% methanol solution. Figure 3 shows measurements of bead width, height of bead,

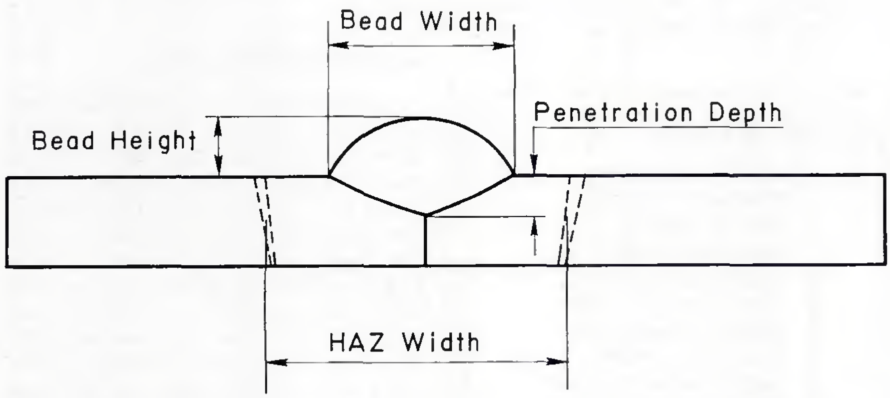

Fig. 3—Metallographic weld sample showing measurements of bead width, height of bead, joint penetration and heat-affected zone.

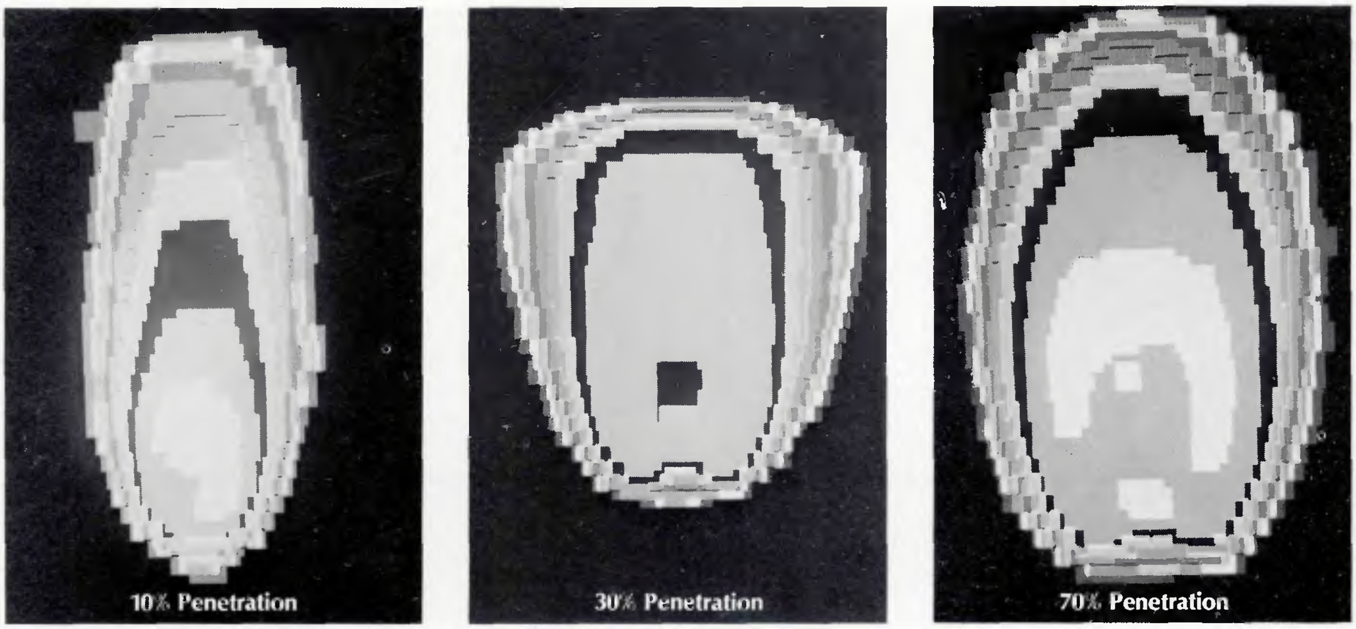

Fig. 4 — Isothermal color plots showing surface temperature distribution information for 10, 30 and 70% joint penetration. (Note: The 10% penetration plot has been enlarged by a factor of 5 to show details of the temperature distribution.)

joint penetration and heat-affected zone that were taken from the metallographic weld samples.

Experimental Results

Figures 4 and 5 show the corresponding temperature distributions obtained during welding, displayed in the form of isotherm color plots and linear line scans for three welds of varying joint penetration (10, 30 and 70%). Different currents were used to produce the penetration variations, holding all other experimental variables constant. From Figs. 4 and 5, one sees that there are identifiable changes in surface temperature distributions. The changes occur in peak temperature of the weld pool, width of temperature peak, area under the temperature distribution and gradient of temperature as a function of distance. Figure 6 shows how each of these thermal profile characteristics were extracted from the thermal image. Each of these identifiable changes in the temperature distribution may be associated with one or more changes in the weld being produced.

One of the more easily identifiable weld process perturbations is bead width. The bead width should be directly proportional to the width of the temperature peak that represents molten metal bead size, the proportionality being a scale factor for camera angle/viewing lens magnification. A computer routine was developed to measure the bead width based on the surface temperature distributions obtained. Individual temperature vs. distance scans (perpendicular to welding gun travel) of a single frame of information were first analyzed to determine the profile with the largest peak temperature. Furthermore, this temperature vs. distance profile was then used to calculate the width of the temperature peak by measuring the profile width at the temperature midway between the peak and background temperature. Figure 7 shows the relation between width of bead and half-height width in pixels of the temperature distribution. As anticipated, a linear relationship exists.

From the peak temperature vs. distance profile used in the above calculation of the midtemperature width, the area under the temperature distribution was calculated.

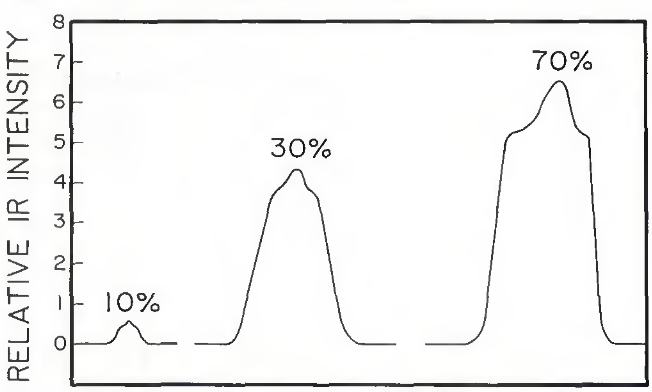

Fig. 5 — Temperature vs. distance scans of data from Fig. 4 for 10, 30 and 70% joint penetration.

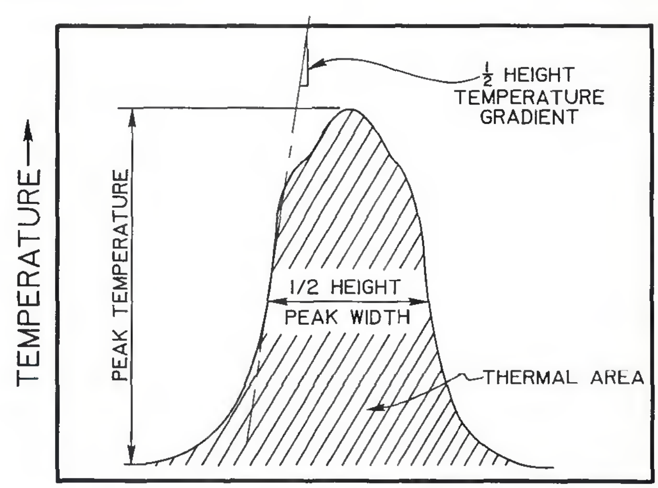

Fig. 6 — Diagram showing thermal scan characteristics used to evaluate joint penetration.

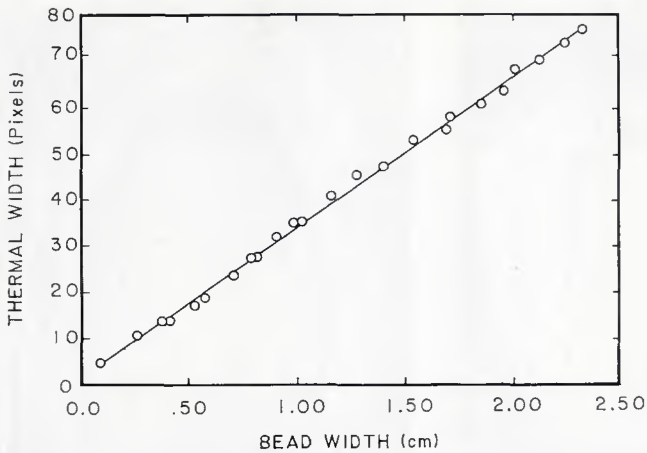

Fig. 7 — Relationship between bead width and width of thermal peak of the temperature distribution.

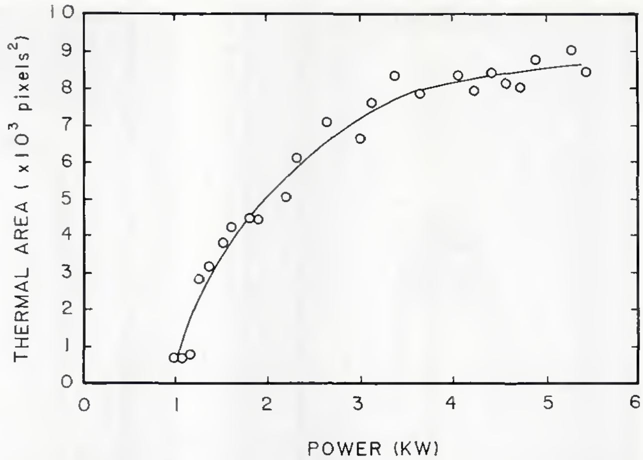

Fig. 8 — Relationship between the area under the temperature distribution and the power generated by the weld power supply.

This integrated area should be a measurement of the heat input into the weld. If one assumes heat loss conditions are proportional to the power applied, then a relationship between the power generated by the welding power source and area under the temperature distribution should exist. Figure 8 shows that a repeatable relationship does exist between the area under the temperature distribution and the power generated by the welding supply.

Figure 9 shows there is a relationship between the depth of joint penetration and the area under the peak temperature profile. When the data of Fig. 9 are plotted in the form of a log-log plot (Fig. 10) a linear relationship is found between the penetration and area under the temperature curve. This behavior is not surprising since the area under the peak temperature curve increases with power — Fig. 8. The joint penetration is found to be highly sensitive to the area under the peak temperature distribution at high values of penetration (above 25%), with the sensitivity decreasing with decreasing penetration. However, the scatter of the data and sensitivity of the relationships between joint penetration and area under the peak temperature distribution appear to be adequate to attempt feedback-controlled penetration during GMA welding.

Discussion

Using an infrared technique to monitor the surface temperature distributions during the welding process is a sensitive, fast and convenient method that may be applicable to adaptive control of the welding process. The results of this set of experiments show that the technique discussed might be used to control depth of joint penetration and bead width during the GMA welding process. Efforts are underway to test this concept of penetration control by increasing or decreasing power automatically.

One of the flaws of infrared thermography is that absolute temperatures are a function of surface emissivity, which varies from material to material, of surface preparation and surface temperature itself. The results presented in this paper do not rely on absolute temperature, but on relative temperature with respect to a specific chosen temperature on the plates.

Conclusions

The following conclusions resulted from this study:

1) Infrared thermography may be applicable to adaptive control of joint penetration and bead width during GMA welding of steel.

2) A linear relationship exists between the width taken at the midtemperature of the peak temperature profile during the welding process and the bead width.

3) An exponential relationship exists between the depth of joint penetration and integrated area under the peak temperature profile obtained during the welding process.

Acknowledgments

The authors express their thanks to the Dept. of Energy for sponsoring this project

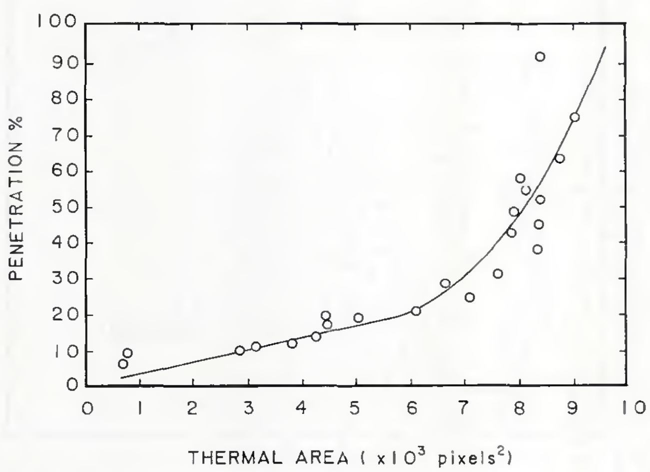

Fig. 9 — Relationship between joint penetration and the area under the peak temperature profile.

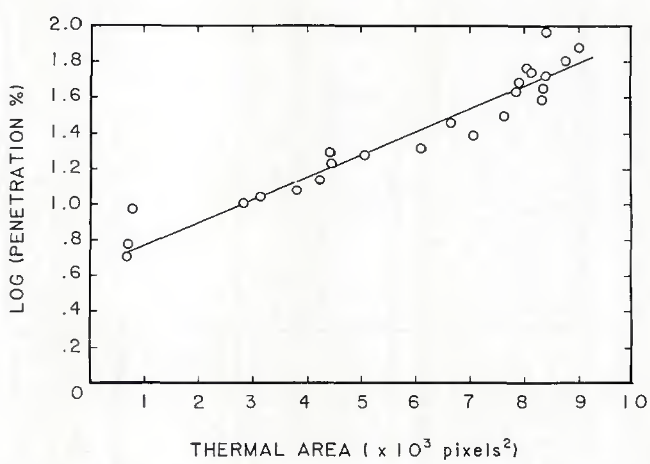

Fig. 10 — Data of Fig. 9 become linear when plotted as log penetration % vs. thermal area.

under grant DE-FG07-88ER12817-90, and for collaborative research travel sponsored in part by the Div. of Materials Sciences, U.S. Dept. of Energy, through the SHaRE program under contract DE-AC05-76ORO0033 with Oak Ridge Associated Universities.

References

1. L'vov, M. S., and Igoshin, A. P. 1971. A system for the automation of arc welding with self-adjustment by depth of penetration. *Automatic Weld* 24(5):35.

2. Vroman, A. R., and Brandt, H. 1976. Feedback control of GTA welding using puddle width measurement. *Welding Journal* 55(9) 742–749.

3. Friedman, E. 1978. Analysis of weld puddle distortion and its effect on penetration. *Welding Journal* 57(6):161-s to 166-s.

4. Savage, W. F., Nippes, E. F., and Zanner, F. J. 1978. Determination of GTA weld-puddle configurations by impulse decanting. *Welding Journal* 57(7):201-s to 210-s.

5. Glickstein, S. S., and Yeniscavich, W. 1977. A review of minor element effects on the welding arc and weld penetration. *WRC Bulletin No. 266.*

6. Correa, S. M., and Sundell, R. E. 1986. A computational and experimental study of the fluid flow in weld pools. *Proceedings of the Engineering Foundation Conference on Modeling and Control of Casting and Welding Processes,* Santa Barbara, Calif.

7. Sundell, R. E., *et al.* 1986. Minor element effects on gas tungsten arc weld penetration. *General Electric Report No. 86SRD013.*

8. Chin, B. A., Madsen, N. H., and Goodling, J. S. 1983. Infrared thermography for sensing the arc welding process. *Welding Journal* 62(9):227-s to 234-s.

9. Wang, Yuwen, and Chin, B. A. 1986. Online sensing of weld penetration using infrared thermography. SPIE Vol. 665, *Optical Techniques for Industrial Inspection,* pp. 314–320.

10. Nagarajan, S., Chen, W. H., and Chin, B. A. 1989. Infrared sensing for adaptive arc welding. *Welding Journal* 68(11):462-s to 466-s.